Published in final edited form as:
Mol Microbiol. 2010 June ; 76(6): 1340–1357. doi:10.1111/j.1365-2958.2010.07181.x.

Cathepsin L Occupies a Vacuolar Compartment and is a Protein Maturase within the Endo/Exocytic System of *Toxoplasma gondii*

Fabiola Parussini[1], **Isabelle Coppens**[2], **Parag P. Shah**[3], **Scott L. Diamond**[3], and **Vern B. Carruthers**[4,*]

[1]Department of Microbiology and Molecular Genetics, University of Vermont, Burlington, VT 05405 U.S.A.

[2]Department of Molecular Microbiology and Immunology Johns Hopkins University School of Public Health , Baltimore, Maryland 21205 U.S.A.

[3]Institute for Medicine and Engineering, Penn Center for Molecular Discovery, University of Pennsylvania, Philadelphia, Pennsylvania 19104 U.S.A.

[4]Department of Microbiology and Immunology, University of Michigan, Ann Arbor, Michigan 48109 U.S.A.

Abstract

Regulated exocytosis allows the timely delivery of proteins and other macromolecules precisely when they are needed to fulfill their functions. The intracellular parasite *Toxoplasma gondii* has one of the most extensive regulated exocytic systems among all unicellular organisms, yet the basis of protein trafficking and proteolytic modification in this system is poorly understood. We demonstrate that a parasite cathepsin protease, TgCPL, occupies a newly recognized vacuolar compartment (VAC) that undergoes dynamic fragmentation during *T. gondii* replication. We also provide evidence that within the VAC or late endosome this protease mediates the proteolytic maturation of proproteins targeted to micronemes, regulated secretory organelles that deliver adhesive proteins to the parasite surface during cell invasion. Our findings suggest that processing of microneme precursors occurs within intermediate endocytic compartments within the exocytic system, indicating an extensive convergence of the endocytic and exocytic pathways in this human parasite.

Keywords

limited proteolysis; protein trafficking; regulated secretion; cell invasion; endocytic pathway

Introduction

Proteins destined for regulated exocytosis navigate through complex intramembranous pathways prior to their release from the cell. Such pathways employ mechanisms for protein sorting, vesicle budding, processing of secretory protein precursors (termed proteolytic maturation), and stimulus-dependent membrane fusion. Several models have been proposed for the main branch point where proteins are segregated for exocytosis. The conventional model proposes that the trans-Golgi network (TGN) is the principal sorting station where

*Corresponding author. Mailing address: Department of Microbiology and Immunology, University of Michigan School of Medicine, 1150 W. Medical Center Drive, Ann Arbor, MI 48109. Phone: (734) 763-2081. Fax: (734) 764-3562. vcarruth@umich.edu.

targeting signals are recognized by cargo receptors that steer proteins toward the regulated pathway (reviewed in Gu *et al.*, 2001). However, two more recent models hypothesize that additional sorting can occur within post-Golgi compartments. The first post-Golgi sorting model postulates that immature secretory granules emerge from the TGN carrying incompletely segregated populations of secretory proteins and that stowaway proteins are thereafter removed in clathrin-coated vesicles (reviewed in Molinete *et al.*, 2000; Schrader, 2004). The second post-Golgi model proposes that sorting of some proteins takes place in endosomal compartments located distal to the TGN (reviewed in Rodriguez-Boulan *et al.*, 2005; Stow *et al.*, 2009). These models are not mutually exclusive since sorting can occur at multiple sites within any one cell type.

Toxoplasma gondii is a genetically tractable protozoan that is considered a model for intracellular parasitism. For cell invasion and intracellular survival, *Toxoplasma* tachyzoites (the stage responsible for acute infection) critically rely on the sequential regulated discharge from distinct specialized secretory organelles called micronemes, rhoptries, and dense granules (see Fig. 1B for an illustration of the parasite). These organelles supply proteins necessary for parasite apical attachment, formation of a tight binding zone (moving junction), and remodeling of the parasitophorous vacuole in which the parasite replicates (Reviewed in Carruthers *et al.*, 2007; Sinai,2008). Although it is well established that the exocytic system of *T. gondii* and other apicomplexan parasites is highly polarized with secretion occurring from the apical region, precisely what path(s) secretory proteins use to reach the distinct apical secretory organelles remains poorly defined. The endocytic system of *Toxoplasma gondii* is also poorly characterized, principally because of the lack of known endocytic ligands and membrane associated-surface receptors, and the inaccessibility of the parasite to endocytic tracers when it is replicating intracellularly. Nonetheless, several studies suggest that the endosomal system of *T. gondii* is used for both macromolecule uptake and trafficking of invasion proteins to micronemes and rhoptries. For example, fluid phase and membrane endocytic tracers are internalized into putative endosomal compartments of a small subset of isolated parasites indicating that endocytosis occurs at least to some extent under extracellular conditions (Nichols *et al.*, 1994;Botero-Kleiven *et al.*, 2001). Also, over-expression of a constitutively active TgRab5 associated with early endosomes (EE) increases cholesterol acquisition from the host, implying a role in uptake (Robibaro *et al.*, 2002). For exocytic protein trafficking, tyrosine-based endosomal sorting signals (YXXf, where X is any aa and f is bulky hydrophobic aa) and associated adaptor complexes facilitate trafficking from a “pre-rhoptry” compartment to mature rhoptries and from an unidentified post-Golgi compartment to micronemes (Hoppe *et al.*, 2000b). Similarly, a dileucine (LL) motif is thought to aid TgROP2 protein transfer from a endocytic compartment to the mature rhoptries (Ngo *et al.*, 2003;Yang *et al.*, 2004). Several studies have shown that additional sorting signals are contained with the cleavable propeptides of at least four microneme proteins (TgM2AP, TgMIC3, TgMIC5 and TgSUB1; Harper *et al.*, 2006;Binder *et al.*, 2008;Brydges *et al.*, 2008;El Hajj *et al.*, 2008) and one rhoptry protein (TgROP1; Bradley *et al.*, 2001). Finally, antibodies to the propeptides of TgM2AP and TgMIC5 label a vesicular structure termed the ‘VP1 compartment’ positioned near the TGN and EE, but also extending further toward the apical end of the parasite (Harper *et al.*, 2006;Brydges *et al.*, 2008). These findings imply that proteolytic maturation of apical invasion proteins in *T. gondii* occurs within the endosomal system prior to or coincident with packaging into the secretory organelles. Nonetheless, little is known about the properties of *T. gondii* endocytic compartments or precisely how apical invasion proteins are processed and sorted to their final destination within the parasite.

The most widely described roles for proteolytic maturation of proproteins are to modulate protein activity or enhance protein association for packaging into regulated secretory granules. These themes appear to also occur in *T. gondii*. For example, proteolytic

maturation of the adhesive protein TgMIC3 unmasks the receptor binding activity of its lectin-like domain, which is required for normal parasite virulence (Cerede *et al.*, 2002). Also, a maturation resistant mutant of TgM2AP failed to remain stably associated with the adhesive protein TgMIC2, and as a consequence these proteins are secreted inefficiently and the parasite is less invasive (Harper *et al.*, 2006). Given the key sorting and regulatory functions of propeptides, the identification and characterization of the proteolytic maturases responsible for propeptide cleavage may open novel avenues for disrupting secretory protein function.

Herein we show that a parasite cathepsin L-like protease, TgCPL, resides within a previously unrecognized organelle that might be the parasite's equivalent of a lysosome or lytic vacuole. Moreover, we provide evidence that TgCPL is a maturase for at least two micronemal precursor proteins within the *T. gondii* exocytic pathway. Our findings further support the notions that the exocytic and endocytic pathways in *Toxoplasma gondii* are closely intertwined and that a classically degradative lysosomal protease can function in the limited proteolysis of secretory proteins.

Results

TgCPL occupies a discrete apical compartment

TgCPL is a cathepsin L protease related to *Plasmodium falciparum* falcipains, which are best known for their role in hemoglobin digestion during replication in erythrocytes. The precursor form of TgCPL is predicted to be a type II membrane protein based on the presence of a signal anchor domain (Fig. S1), and the mature form contains the key catalytic residues, consistent with it having proteolytic activity (Huang *et al.*, 2009; Larson *et al.*, 2009). While TgCPL has been recently reported to occupy an apical compartment (Huang *et al.*, 2009; Larson *et al.*, 2009), the precise nature of this compartment or its relationship to other apical structures has not been investigated. To determine if TgCPL is associated with the parasite endocytic and/or exocytic system, we examined its subcellular distribution compared to other established markers within tachyzoites using specific antibodies to TgCPL (Fig. S1). In extracellular and newly invaded parasites, TgCPL displayed a discrete pattern that was typically confined to one or two structures within the apical region (Fig. 1Ai-ii). The structure was occasionally seen posterior to the nucleus but only in a minority of parasites (<10%), and it was often visible as a vacuole-like structure by phase contrast microscopy (data not shown). Intracellular replicating parasites often showed a greater number of smaller labeled structures distributed throughout the cytoplasm (Fig. 1Aiii). TgCPL was typically located near but distinct from the apical rhoptries and pre-rhoptries (Fig. 1B) (Carey *et al.*, 2004). TgCPL localization was also distinct from the recently described cytoplasmic aggregate of dynamin related protein B (DrpB) (Breinich *et al.*, 2009). Some colocalization of TgCPL was seen with the micronemal protein TgAMA1, indicating a possible link to the microneme pathway. The TgCPL-associated structure was often positioned anterior to the parasite's single Golgi apparatus, and in close juxtaposition to the apicoplast (a remnant plastid seen in most apicomplexan parasites). Interestingly, TgCPL was also located near the EE marker TgRab51 (Robibaro *et al.*, 2002). Together these findings suggest that TgCPL defines a unique structure that is distinct from other apical organelles, but one that seems affiliated with the microneme exocytic pathway and the endosomal system. Moreover, TgCPL is localized in a similar structure in the bradyzoite stage (Fig. S2A), a slow growing developmental form of the parasite responsible for chronic infection. Because of its unique properties and appearance, we termed this structure the vacuolar compartment or VAC.

The VAC is juxtaposed to the late endosomes

To better characterize the relationship of the VAC with the endosomal system of *T. gondii*, we next performed immunolocalization studies in intracellular tachyzoites transiently transfected with a plasmid expressing an epitope tagged copy of *T. gondii* Rab7 homologue (TgRab7). In other eukaryotes Rab7 is principally associated with late endosomes (LE) where it regulates vesicular traffic to the lysosome or vacuole (Mullock *et al.*, 1998). *T. gondii* expresses a single Rab7 (TGME49_048880, www.toxodb.org) that is homologous to Rab7 proteins from other eukaryotes and has the functionally important regions of a small GTP-binding protein, including the effector binding region, four GTP-binding/hydrolysis regions, and C-terminal Cys residues for membrane association via prenylation, (Fig. S3).

Figure 2A (upper panels) shows that TgRab7HA is associated with vesicles positioned anterior to the parasite nucleus and adjacent to the VAC with small areas of partial overlap. To further extend the characterization of this putative LE we performed dual immunolocalization studies with proTgM2AP and the vacuolar proton pump TgVP1, which have been described to co-localized within a post-Golgi structure termed the ‘TgVP1 compartment” (Harper *et al.*, 2006). Figure 2A (middle and lower panels) shows that TgRab7 co-localized extensively with proTgM2AP and TgVP1, albeit with non-identical distributions therein, indicating the presence of substructures or microdomains, a common feature for eukaryotic LE compartments (Pfeffer,2001; Wilkin *et al.*, 2004; Sobo *et al.*, 2007). These findings suggest that the ‘VP1 compartment’ where microneme precursor proteins reside prior to proteolytic maturation is part of the endosomal system and is likely a LE.

Since TgCPL is most easily visualized in extracellular parasites but HA-TgRab7 expression was not well tolerated therein, we used TgVP1 as a surrogate marker of the LE to further investigate its spatial relationship with the VAC. As mention above, TgVP1 is a member of the vacuolar proton pump family that derives energy from the hydrolysis of inorganic pyrophosphate to acidify intracellular compartments including digestive (Zhen *et al.*, 1994) or contractile vacuoles (Montalvetti *et al.*, 2004), acidocalcisomes (Montalvetti *et al.*, 2004), or the trans-Golgi network (Mitsuda *et al.*, 2001). Most parasites (~80%) showed a single apical VAC with some TgVP1 concentrated around the periphery of and adjacent to the organelle (Figure 2B upper two panels). In the remainder of the parasites, the VAC and LE were spatially distinct but each often contained small amounts of the reciprocal marker (Figure 2B lower two panels). Miranda et. al. (accompanying article) show that the VAC also labels with antibodies to TgVP1 and other novel markers.

Ultrastructural analysis of the VAC

Labeling of ultrathin cryosections with anti-TgCPL immunogold showed that the VAC is a large electron lucent structure that resembles a vacuole. The VAC often contained internal vesicles (Fig 3A, A’, A”) and electron dense material lining its periphery (Fig. 3B), both of which were labeled with TgCPL antibodies. TgCPL (~5% of the particles) was also seen in small electron dense structures, possible transport vesicles, throughout the cytoplasm and adjacent to the VAC (Fig. 3A-D). Densely labeled invaginations within the VAC were also observed (Fig. 3C-C’) in addition to outward deformations (Fig. 3D) and tubules (Fig. 3E), illustrating the apparent dynamic nature of the structure and possible conduits to other endosomal structures. Collectively, these observations suggest that the VAC is a dynamic low-density organelle with internal and external vesicles and tubules.

The VAC fragments during parasite intracellular replication

The marked difference in the distribution of TgCPL in extracellular versus intracellular replicating parasites prompted us to examine the basis of this change. Because attempts to

visualize the VAC using TgCPL fused to fluorescent proteins were unsuccessful due to mistargeting and proteolysis of the reporter, we instead examined TgCPL localization by immunoflorescence in fixed parasites at different times post-invasion. *T. gondii* replicates by endodyogeny, a process in which two daughter parasites develop within a mother cell. Progression through the cell cycle was assessed using parasites expressing EGFP-Centrin2 (Hu *et al.*, 2006), a marker of the centrosome that permits recognition of parasites in G1 (single centrosome, anterior in early G1, lateral while migrating to the posterior of the nucleus in late G1), S phase (dual closely-juxtaposed centrosomes, variable position as they migrate back to the anterior), and mitosis (dual separating centrosomes, bilobed nucleus). Parasites undergoing mitosis or cytokinesis were also visualized by staining the inner membrane complex (IMC), which demarcates daughter parasites (Mann *et al.*, 2001). The series of images in Figure 4 shows that the VAC undergoes marked morphological changes during endodyogeny. Early in G1 (0-2 h post-invasion; Fig. 4A, A'), the VAC is small, round and usually located anterior to the nucleus. This is similar to extracellular parasites except that a greater percentage of G1 parasites showed more than one VAC. Later in G1 (2-4 h post-invasion; Fig. 4B-D), the TgCPL staining pattern adopts an enlarged ring shape or is concentrated in patches at the periphery of the VAC, and the volume of the compartment appears to increase. In S phase (4-6 h post-invasion Fig. 4E, F, F'), tubulovesicular structures extend from the VAC following duplication of the apicoplast and expansion of the mother cell. During mitosis (~7 h post-invasion; Fig. 4G-J) when daughter cells begin to form, the VAC seems to fragment into multiple smaller structures. This stage is also characterized by the apparent migration of these smaller structures toward the posterior end of the mother as nuclear division proceeds (Fig. 4J'). Finally, during cytokinesis (7-8 h post-invasion; Fig. 4K, L) when mitosis is complete and the daughter cells are budding from the mother, TgCPL is usually associated with a single structure in the apical end of each daughter cell and in some cases with the residual body located at the posterior end of the mother cell (Fig. 4K'). Quantification of the TgCPL staining patterns during parasite replication (Fig. 4M) shows the apparent progression of the VAC from a small round structure that enlarges and fragments before being seen again often as a single structure within daughter parasites or the residual body. Analysis of TgCPL and TgVP1 distribution during parasite cell division indicates that the VAC and LE remain distinct but often closely associated through each phase of the cell cycle (Fig. S4) and that the LE elongates before being partitioned into the daughter cells (Fig. S5) in a manner similar to the Golgi (Pelletier *et al.*, 2002).

T. gondii cathepsin cleavage subsite specificity is consistent with processing of several proMICs

With the finding that TgCPL is associated with the endocytic system and possibly the microneme pathway, we reasoned that it is in a suitable position to act as a maturase for proMICs, which have been proposed to undergo maturation within the endocytic system (Harper *et al.*, 2006; Brydges *et al.*, 2008; El Hajj *et al.*, 2008). To initially test this we used two approaches to determine whether the cleavage site specificity of TgCPL is consistent with the known cleavage sites of proMICs. First, we used rTgCPL to screen a peptide substrate library to determine its cleavage site preferences. Recombinant TgCPL displayed a strong preference for substrates with a non-polar residue (Val or Leu) or aromatic residue (Phe, Trp, or Tyr) in the P2 position (i.e., the second residue N-terminal to the cleavage site) (Fig. 5A), which is the dominant recognition site for C1 family cathepsins (Barrett, 1981; Turk *et al.*, 1997). Variable preferences were seen for the P3 position. Comparison with human cathepsin L (Gosalia *et al.*, 2005) revealed that, despite organism differences, the fundamental P2 and P3 substrate preferences are remarkably similar, likely reflecting the conventional active site architecture of TgCPL (Huang *et al.*, 2009; Larson *et al.*, 2009). For further comparison we also tested rTgCPB, which showed preferences similar to rTgCPL

except that it can accept additional non-polar or polar uncharged residues such as Ser, Met, and Thr in the P2 position and it has a marked preference for Pro in the P3 position (Fig. 5B).

Second, we performed N-terminal microsequencing of rTgCPL after autoactivation from r100proTgCPL (Fig. S6) to define its self-cleavage specificity. This showed that autocleavage occurs at two sites (L198 and N199), both displaying a hydrophobic residue (Leu) in the P2 position (Fig. 5C). Interestingly, propeptide cleavage sites for several proMICs resemble one another and also display a hydrophobic residue in the P2 position including most notably TgM2AP (Leu), TgMIC6 (Leu), and TgMIC3 (Val). Cleavage sites for TgAMA1 and TgSPATR show some conservation, but the P2 Ala in both proteins is not consistent with cleavage by TgCPL. Similarly, the cleavage sites of proTgMIC5 and proTgMIC11 are very different, making them poor candidate substrates for TgCPL. We conclude from this analysis that the best potential substrates for TgCPL are proTgM2AP, proTgMIC3, and proTgMIC6.

Parasites deficient in TgCPL show impaired maturation of proTgM2AP and proTgMIC3

To more directly determine if TgCPL is a maturase for microneme proteins, we performed a pulse-chase immunoprecipitation analysis of proMIC processing in WT (RH) and TgCPL-deficient (RHΔ*cpl*) parasites (Larson *et al.*, 2009). Consistent with a role in processing, RHΔ*cpl* parasites showed a delay in maturation of proTgM2AP and proTgMIC3 (Fig. 6A-C, Table 1) that significantly shifted the time at which one half of the precursor is processed to product ($T_{1/2}$) from ~37 min to 56 or 48 min, respectively (Table 1). That processing was not abolished completely suggesting the existence of alternative maturases. Processing of TgMIC5 (data not shown), TgMIC6, or TgAMA1 was not affected in RHΔ*cpl* (Fig. 6D-E), indicating the absence of a global effect on microneme protein trafficking or function. Since TgM2AP and TgMIC3 both contribute to cell invasion (Huynh *et al.*, 2003; Cerede *et al.*, 2005), we assessed the invasion proficiency of RHΔ*cpl* parasites using a differential staining assay capable of distinguishing extracellular attached parasites from intracellular invaded parasites (Huynh *et al.*, 2003). These experiments showed that RHΔ*cpl* parasites are 50-60% less invasive than RH (Fig. 6F). While it is unclear whether this invasion phenotype is due entirely to the defects in TgM2AP and TgMIC3 maturation, the finding is consistent with previously observed synergistic effects of deficiencies in multiple microneme proteins (Cerede *et al.*, 2005).

rTgCPL processes rproTgM2AP at the correct cleavage site in vitro

To determine if TgCPL can correctly execute proTgM2AP maturation *in vitro*, we incubated rTgCPL with rproTgM2AP in buffers of increasing pH and examined products of the reaction over time (Fig. 7A). As expected of a cathepsin protease, rTgCPL processing of rproTgM2AP did not occur at neutral pH but was most evident at pH 5.5-6.5. Similar results were seen for autocatalytic activation of r100TgCPL (Fig. S4). The TgM2AP proteolytic product comigrated with a recombinant TgM2AP product (rTgM2AP) that mimics mature TgM2AP, suggesting that cleavage occurred at or near the correct processing site. This was confirmed by N-terminal microsequencing of the product, yielding the sequence T-F-L-E-D, which is identical to that of mature TgM2AP isolated from parasites (Fig. 5C) (Rabenau *et al.*, 2001). These findings establish that TgCPL is capable of processing TgM2AP in a low pH dependent manner at precisely the same cleavage site used *in vivo*.

Maturation of TgCPL and its substrates are differentially sensitive to pH agonists *in vivo*

Having confirmed that rTgCPL activity requires low pH *in vitro*, we next used pH modulating treatments to test whether processing of native TgCPL and the substrates proTgM2AP and proTgMIC3 is also pH dependent *in vivo*. Extracellular parasites were

pretreated with increasing concentrations of bafilomycin A1 (a specific inhibitor of vacuolar-type H(+)-ATPase) or chloroquine (a weak base that neutralizes acidic organelles) and subjected to pulse-chase immunoprecipitation. Without treatment, processing of proTgCPL (50 kDa) to TgCPL (30 kDa) proceeded with $T_{1/2}$ ~30 min and was mostly complete by 60 min (Fig. 8A). Interestingly, proTgCPL processing was largely resistant to bafilomycin A1 or chloroquine treatment, with inhibition seen principally at the highest concentrations tested (500 nM and 150 μM, respectively). Intermediate processed forms of TgCPL (48 kDa and 32 kDa) were seen, indicating that proTgCPL undergoes at least three processing steps during maturation. In contrast, maturation of proTgM2AP and proTgMIC3 was much more sensitive to treatment, with complete inhibition at concentrations ~10-fold lower than for TgCPL (Fig. 8B). Thus, although processing of proTgCPL and its substrates both require low pH (see also Fig. S6), they are differentially sensitive to pH antagonists.

To determine if the pH antagonists bafilomycin and chloroquine affect morphology of the VAC and LE, we treated extracellular parasites with increasing concentrations of these compounds and subjected them to IFA analysis. The Golgi was visualized by detection of TgGRASP-mRFP as control and to determine the polarity of the parasites. Consistent with the previous findings, without treatment the VAC and LE are located in the apical end of the parasites; the VAC is round, and the LE shows a discrete pattern confined to one or two punctuate structures (Fig. 8C-D, upper panels). However, when the parasites where pretreated with chloroquine or bafilomycin A1 at the same range of concentrations used above, the sizes of the VAC and LE increased (Fig. 8C-D, middle and lower panels; Fig. S7A-B). Additionally, treatment with 150 μM chloroquine appeared to cause dispersal of the LE into smaller structures seen at both ends of the parasites (Fig 8D, lower panel; Fig. S7B). Although we cannot rule out indirect effects of the treatment, the observed morphological changes could be due to disruption of pH-dependent physiological processes within the VAC and LE including the activities of ion transporters and water channels, both of which are associated with these compartments (Miranda et al., accompanying article). In contrast, the size and shape of the parasite Golgi remained unchanged at all drug concentrations tested (Fig. 8C-D). Together, these findings suggest that the TgCPL-associated endosomal compartments are acidified, which is consistent with pH sensitive processing of proMICs and proTgCPL therein.

TgCPL and proTgM2AP encounter each other discretely within the endocytic system

To further test whether processing of proMICs occurs within the endocytic system, we next examined the distribution of TgCPL and proTgM2AP during and after replication. The series of images in Figure 9A shows that during G1 phase proTgM2AP is mainly concentrated in the LE and a small amount of the precursor colocalized with TgCPL at specific areas of the VAC (arrow). In S phase, proTgM2AP is distributed in a tubulovesicular pattern and small areas of overlap with TgCPL are still evident (arrows). Interestingly, during mitosis (data not shown) when the VAC is fragmented, the level of proTgM2AP decreased and was no longer detectable until cytokinesis where proTgM2AP is associated with a LE compartment in closed association with the VAC. It is unclear whether the transient disappearance of proTgM2AP is due to an interruption in its synthesis or an increase in the efficiency of processing to mature TgM2AP. Extracellular parasites showed a similar pattern as G1 parasites with small areas of TgCPL and proTgM2AP colocalization. Cryoimmunoelectron microscopy revealed that TgCPL (10 nm gold) along with proTgM2AP (5 nm gold; Fig. 9B) or TgM2AP (5 nm gold; Fig. 9C-E) co-inhabited electron lucent structures where they were associated with internal electron dense material at the periphery. Micronemes, identified based on their size and shape, were often seen adjacent to these structures (Fig. 9B, D, and E). Although some of these lucent structures showed internal vesicles similar to those of the VAC, this does not exclude the possibility of them

being the LE. Indeed, in some examples two TgCPL labeled structures were seen (Fig. 9E) with the structure on the left containing TgM2AP and some TgCPL, consistent with the LE, and the structure on the right containing little or no TgM2AP and substantially more TgCPL, indicative of the VAC. Interestingly, micronemes are seen adjacent to the putative LE, with the most proximal micronemes containing both TgM2AP and TgCPL and the distal micronemes in the upper portion of the image containing principally TgM2AP. This is suggestive of TgCPL entry into nascent micronemes before being recycled back to the endosomal compartment (LE or VAC).

Discussion

We show that *T. gondii* cathepsin L-like protease, TgCPL, is associated with endocytic organelles, including most prominently a VAC that is distinct from other well known apical organelles of *T. gondii*. Given is location proximal to the LE marked by TgRab7 and TgVP1, it is reasonable to consider that the VAC is the *T. gondii* equivalent of a lysosome or lytic vacuole. Few studies have attempted to identify lysosome-like organelles in this parasite, and the findings are varied. Norrby et. al. (Norrby *et al.*, 1968) showed that acridine orange, a fluorescent dye that accumulates in acidic structures, labels small vesicular structures within extracellular and intracellular parasites. The same study showed the presence of multiple black spots in intracellular tachyzoites stained with the Gomori technique for lysosomes, and that these structures increased with time after invasion. However, using the acidotropic agent DAMP and electron microscopy, Shaw *et. al*. (Shaw *et al.*, 1998) failed to detect a lysosomal-like compartment. This study did, however, suggest that pre-rhoptries and mature rhoptries are acidic and this, along with a series of studies by Keith Joiner's group (Hoppe *et al.*, 2000a; Hoppe *et al.*, 2000b; Ngo *et al.*, 2003), led to the idea that rhoptries are secretory lysosomes (reviewed in Ngo *et al.*, 2003). Our findings along with those of Miranda et al (accompanying article) strongly suggest that *T. gondii* has an endolysosomal system that includes at least one typical lysosomal protease, TgCPL.

We also showed that the VAC is a dynamic organelle that undergoes a cell cycle dependent fragmentation process. This phenomenon is reminiscent of the inheritance mechanism used by*Saccharomyces cerevisiae* to actively distribute organelles into the budding cell. Early in the yeast cell cycle a portion of the mother cell organelles, including the vacuole, mitochondria, the endoplasmic reticulum (ER), late-Golgi elements and peroxisomes are actively transported to the budding daughter cell (reviewed in (Weisman, 2006)). We show that tubulovesicular projections from the VAC appear immediately before daughter cell formation. With the current view it is not possible to distinguish whether the small TgCPL positive structures are migrating into the new daughters or are instead moving toward the posterior end of the mother cell to possibly function in catabolism of proteins in the residual body. It is also not clear if the organelle fragmentation and movement is part of a regulated mechanism to modulate and coordinate the function of the VAC with the cell cycle of the parasite. Gaining further insight into the dynamics of VAC fragmentation will require new markers of the VAC suitable for fluorescent tagging and live cell visualization during intracellular replication.

Huang et. al. also partially characterized TgCPL (Huang *et al.*, 2009). Our findings extend this work by showing that TgCPL occupies the internal periphery of the VAC, and that it contributes to the maturation of proMICs during trafficking to the micronemes. Whereas the previous report found that recombinant TgCPL is most active at pH 6.0-6.5 (Huang *et al.*, 2009), we our findings indicate its activity is maximal at pH 5.5. This may reflect the use of different substrates since Huang et. al. used a synthetic peptide substrate while we used proteinaceous substrates including rTgCPL itself (autoactivation) and rproTgM2AP. Huang et. al. also found that rTgCPL cleaves a substrate with P2 Leu approximately two times

better than Phe, and they suggested this was due to Asp216 creating a relatively shallow S2 binding pocket based on a structural homology model of TgCPL (Huang *et al*., 2009). However, the recent reported crystal structure of TgCPL (Larson *et al.*, 2009) showed that Asp216 does not impinge the S2 binding pocket, which is consistent with our finding that substrates with a P2 Leu or Phe are cleaved approximately equally well, albeit with some distinctions due to preferences a the P3 position. The source of the recombinant enzyme, *P. pastoris* (Huang *et al.*, 2009) or *E. coli* (current study), might also influence the catalytic properties of rTgCPL.

Proteolytic maturation is a common feature of regulated secretory pathways. We provide multiples lines of evidence for TgCPL acting as a maturase for at least two microneme precursor proteins, proTgM2AP and proTgMIC3, within a regulated secretory pathway of *T. gondii*. This notion is further supported by the preference of TgCPL for P2 Leu and other hydrophobic residues, which is consistent with the propeptide cleavage sites of several proMICs, and the correct processing of rproTgM2AP by rTgCPL. TgCPL is expressed in bradyzoites along with TgM2AP and TgMIC3 (Fig. S2B-C), thus it also has the potential to act as a maturase in encysted, chronic stage of the parasite. However, maturation of TgM2AP and TgMIC3 was not completely abrogated in the RHΔ*cpl* strain, indicating that at least one additional maturase is capable of processing these substrates. Accordingly, we found that treatment of RHΔ*sub1* parasites with PMSF or subtilisin inhibitor III impair processing of proTgMIC3 (Fig. S8), implying the involvement of an additional subtilisin-like enzyme. Moreover, that TgCPB has very similar substrate preferences to TgCPL could hint to it being responsible for the residual maturation of TgM2AP in RHΔ*cpl* parasites. TgCPB has been reported to occupy the rhoptries and act as a maturase for rhoptry proteins (Que *et al.*, 2002), hence it probably also traffics through the endolysosomal system where it could encounter microneme substrates. However, treatment of RHΔ*cpl* parasites with the cathepsin B inhibitor CA074Me did not affect the maturation of proTgM2AP or proTgMIC3 (data not shown), thus additional experiments will be necessary to clarify the involvement of TgCPB. Maturation of TgMIC6, TgMIC5, TgAMA1, and was not affected in RHΔ*cpl* parasites, providing further evidence of distinct maturases.

To correctly process proMIC substrates without unwanted degradation, TgCPL zymogen activation and protease activity are probably regulated at several levels. We show that the autocatalytic processing of proTgCPL and the maturation of at least two proMICs (proTgM2AP and proTgMIC3) are both pH dependent, albeit in a distinguishable manner. The differential sensitivity to pH antagonists could indicate that TgCPL zymogen activation occurs in a distinct compartment from that of proMIC maturation, thereby segregating these events as a first level of regulation. Moreover, pH modulation by vacuolar H^+-ATPases or other types of proton pumps could be an important secondary factor governing proMIC maturation by TgCPL as well as the activity of alternative maturases. Whether the vacuolar H^+-ATPase-positive structures associated with the VAC (Miranda et. al., accompanying article) are involved in proMIC processing will require further investigation. TgCPL activity might be controlled at a third level by segregation of the protease within intralumenal vesicles of endosomes. It is well established in several eukaryotic systems that multivesicular endosomes like the VAC are dynamic organelles that use intralumenal vesicles to partition storage, recycling, and sorting functions from degradative activities (Woodman *et al.*, 2008). Finally, regulation could be governed by allowing only limited amounts of TgCPL access to proMICs in the processing compartment. The low levels of TgCPL in the LE during microneme biogenesis are consistent with this notion. Stringent regulation would help avoid inappropriate processing or degradation and favor limited proteolysis of proMICs and possibly other substrates.

Our findings imply that the endocytic and exocytic pathways converge in common intermediate compartments for the biogenesis of the micronemes, and possibly other apical organelles. The hypothetical model depicted in Fig. 10 illustrates that after being synthesized in the ER microneme proteins are routed through the Golgi apparatus and transported to micronemes via a series of post-Golgi endosomal compartments including the EE, LE, and possibly the VAC. Rather than the TGN being the site of regulated secretory organelle biogenesis as in many eukaryotic cells, our model predicts that micronemes are derived from the endocytic system, specifically the LE or VAC. The use of endocytic organelles for exocytic trafficking is not without precedent since recent studies have shown that recycling endosomes are used as sorting stations for the exocytosis of, for example, E-cadherin in epithelial cells (Desclozeaux *et al.*, 2008) and the cytokines IL-6 and TNFα in macrophages (Manderson *et al.*, 2007). Our model further predicts that proteolytic maturation of proMICs mediated by TgCPL occurs within the LE and/or VAC. The observation of TgCPL within micronemes proximal to an endosome also raises the possibility of cleavage occurring within nascent micronemes prior to recycling of the protease back to its cognate compartment. In any case, since microneme propeptides contain targeting information (Harper *et al.*, 2006;Brydges *et al.*, 2008;El Hajj *et al.*, 2008), it is expected that these cleavable elements are removed only after they have fulfilled their role in targeting. Precisely where and how they perform this function remains to be determined. Future studies aimed at disabling vesicular transport at specific points in the secretory pathway may help further elucidate the principal sites of proTgCPL and proMIC maturation.

Experimental Procedures

Parasite Culture

T. gondii tachyzoites (RH strain, RHΔcpl, and RH-EGFPcentrin2) were cultured in human foreskin fibroblast cells and isolated as described previously (Harper *et al.*, 2006).

Expression, refolding, and autoactivation of recombinant TgCPL

Procedures for expression, refolding, and autoactivation of recombinant TgCPL are described in detail by Larson *et. al.*, (Larson *et al.*, 2009).

For the analysis of the pH-dependent activation of r100proTgCPL, purified proenzyme was incubated with 100mM sodium acetate or 100mM MOPS buffers each containing 900 mM NaCl, 2 mM EDTA, 5 mM DTT at pH values ranging from 4 to 8 in 0.5 pH increments. Autoactivation proceeded at 37°C, 5 h and was terminated by addition of 5X sample buffer, electrophoresis and staining with 0.1% Coomassie R-250.

For N-terminal sequencing of mature enzyme, 5 μg of processed and purified rTgCPL was subjected to SDS-PAGE, transferred on to PVDF membrane, Coomassie stained, and subjected to Edman sequencing by Midwest Analytical, Inc.

Preparation of antibodies

A synthetic peptide corresponding to TgCPL aa 296-311 (LARDEECRAQSCEKVV) was synthesized and coupled to keyhole limpet hemocyanin (KLH). Rabbits were injected with 200 μg conjugated peptide in Freund's complete adjuvant and boosted 4X at 2-week intervals with 200 μg of conjugated peptide in Freund's incomplete adjuvant. Preimmune serum and 12-week hyperimmune serum was affinity purified with the immunizing peptide using Amino-Link™ beads (Pierce). A polyclonal rabbit antiserum against r100proTgCPL was produced as described above. Mouse anti-r100proTgCPL was made by immunizing mice with a single injection of 25 μg of recombinant protein with TiterMax Gold adjuvant. RαTgCPBpep, which is a rabbit polyclonal antibody to TgCPB aa 550-563

(PGQRAAGARAGAHA) kindly provided by Drs L. David Sibley and Antonio Barragan, was affinity purified with the immunizing peptide as described above.

SDS-PAGE and immunoblotting

Samples were diluted in SDS-PAGE sample buffer containing 2% ß-mercaptoethanol and boiled for 5 min before resolving on 10% or 12.5% SDS-PAGE minigels and semidry-transfer to nitrocellulose membranes, blocking with skim milk and incubating with primary antibodies. Secondary antibodies were either goat anti-mouse- or goat anti-rabbit-conjugated horseradish peroxidase. Blots were visualized with SuperSignal™ West Pico chemiluminescent substrates (Pierce).

Immunofluorescence

Immunofluorescence staining was performed as described previously (Harper *et al.*, 2006). Images were digitally captured using a RT Spot Slider charge-coupled device camera on a Nikon Eclipse E800 microscope at room temperature with a 100X, 1.3 NA oil objective lens. Mowiol was used as the mounting medium. Deconvolution was performed using the no-neighbors algorithm of Simple PCI software (Compix), and final images were assembled using Adobe Photoshop (Adobe Systems).

Cloning and expression of HA-TgRab7

A 0.60-kb fragment encoding TgRab7 (was PCR amplified by PCR from a *T. gondii* RH cDNA library (V.B. Carruthers, unpublished) using primers TgRab7.Nhe I .F (5'-AGTCGCTAGCATGCCGCCCAAGAAGAAGGCTC- 3', *NheI* site underlined) and TgRab7.PacI.R (5' –AGTCTTAATTAATCAGCAGCAGCCGCCGC- 3', *PacI* site underlined) and Expand™ High Fidelity enzyme mix (Roche). The amplicon was gel-purified using a Qiagen gel extraction kit, initially ligated into pGEM-T Easy Vector and transformed into DH5α *E. coli* strain. Clones were sequenced in both directions and digested with the restriction enzymes *Nhe*I and *PacI*.

For *T. gondii* expression, the TgRab7 cDNA was ligated into *NheI* and *PacI* digested pTgRab51HA construct (Robibaro *et al.*, 2002), which provided an in-frame HA tag at the N-terminus, thereby generating pHA-TgRab7. Transient transfections were performed to express HA-TgRab7 in RH strain parasites. For each transfection 75 μg of DNA was used, and immunofluorescence analysis was performed 24 h after transfection.

Metabolic labeling and immunoprecipitation

Freshly lysed tachyzoites were harvested and resuspended in Met/Cys-free DMEM containing 10 mM HEPES pH 7.0, and 2 mM L-Gln. Parasites were preincubated 15 min, RT with solvent control (DMSO) or drug (bafilomycin A, or chloroquine) then pulsed-labeled with 300 μCi [^{35}S] Met/Cys (Amersham Redivue Pro-mix) for 10 min, 37°C and chased in unlabeled medium with 5mM methionine, 5 mM cysteine, and drug for the indicated times. Parasites were washed with medium, resuspended in 0.8 ml RIPA buffer (50 mM Tris pH 7.5, 100 mM NaCl, 5 mM EDTA pH 8.0, 1% Triton X-100, 0.5% sodium deoxycholate, 0.2% SDS, 10 μgml^{-1} RNase A, 20 μgml^{-1} DNase I, and protease inhibitors), incubated 30 min, 0°C, and insoluble material was removed by centrifugation (13,000 rpm, 10 min, 4°C). Antibodies to MIC proteins or TgCPL were incubated with 400 μl of extract for 1 h, 4°C with gentle rocking, followed by addition of 100 μl 10% (v/v) slurry of protein G-sepharose beads, and 1 h incubation, 4°C with gentle rocking. Immune complexes were washed four times with 1ml RIPA buffer before boiling in SDS PAGE sample buffer containing 2% ß-mercaptoethanol, separation by SDS-PAGE, incubation in fluorographic enhancer (Amplify™, Amersham), drying in cellophane, and exposure to X-ray film.

Invasion Assays

Red-green invasion assays were performed as described previously (Huynh *et al.*, 2003).

Expression of rproTgM2AP and rTgM2AP

A 0.68-kb fragment coding for the prodomain and N-terminal β-Sheet domain (aa 23-225) of TgM2AP (rproTgM2AP) was PCR amplified from pET22b/proTgM2AP plasmid (KE Rabenau, unpublished data) using forward M2AP.64.NdeI.F (5'-GATCCATATGGCAAGGAAAGTTGGAAATCCG-3', *Nde*I site underlined) and reverse M2AP.720.NotI.R (5'-GATCGCGGCCGCACTCGGTTCCTCTCCGGC-3', *Not*I site underlined) primers and Expand High Fidelity enzyme mix (Roche). The PCR product was gel-purified using a Qiagen gel extraction kit, ligated into PGEM-T Easy Vector and transformed into DH5α *E. coli* strain. Clones were sequenced in both directions and digested with the restriction enzymes *Nde*I and *Not*I.

For recombinant protein expression, the proTgM2AP-β-sheet domain cDNA was transferred into pET22b (Novagen) using *Nde*I and *Not*I enzyme restriction sites and transformed into competent *E. coli* BL21(DE3) cells (Stratagene) along with pET22b/TgM2AP (consisting of the ß-sheet domain alone; Harper J, unpublished data). Stationary phase bacterial cultures were diluted 1:20 in 100 ml of prewarmed Terrific broth supplemented with ampicillin (100 μgml^{-1}), and grown to mid-log phase. Expression was induced with 0.5 mM IPTG, 3 h and recombinant proteins were purified essentially as described above. Positive fractions were pooled and concentrated and buffer exchanged into 20 mM TrisHCl pH 8.0 using a spin concentrators (AMICON ULTRA-15; Millipore).

Processing of rproTgM2AP-β-sheet domain by rTgCPL

To evaluate processing, 30 μl reactions containing 400 ng of rproTgM2AP and 40ng of rTgCPL were incubated in 100 mM sodium acetate or 100 mM MOPS buffers as described above. Reactions were stopped by addition of 7.5 μl of 5X SDS-PAGE sample buffer and analyzed by immunoblotting.

For N-terminal sequencing of the mature TgM2AP product, 20 μg of rproTgM2AP and 400 ng of rTgCPL were incubated with 100 mM sodium acetate buffer containing 900 mM NaCl, 2 mM EDTA, and 10 mM DTT pH 5.5 at 37°C for 5 min (300 μl final volume). E64 (100 μM final) was added to stop the reactions, and the sample was concentrated to 50 μl, run on SDS-PAGE, transferred on to PVDF membrane, and Coomassie stained. The TgM2AP product band was excised and subjected to Edman sequencing as above.

In vitro bradyzoite differentiation

Fibroblasts were infected with ME49 or Pru strain tachyzoites in MEM without $NaHCO_3$ but containing 25 mM HEPES and incubated in low CO_2 (0.03%) for 3 to 5 days (Matrajt *et al.*, 2002). Infected monolayers were fixed with 4% paraformaldehyde, permeabilized in 0.1% Triton X-100 for 15 min, and blocked with 10% FBS for 30 min. Primary antibodies were diluted in PBS containing 1% FBS/1%NGS and incubated for 1h. Secondary antibodies (AlexaFluor 488 goat anti-mouse or goat anti rabbit) were incubated for 1 h before washing three times, rinsing with PBS, and mounting. The bradyzoite cyst wall was labeled with TRITC-conjugated *Dolichos biflorus* lectin.

Acknowledgments

We thank Matthew Bogyo, Carolyn Phillips, Silvia Moreno, and Sharon Reed for helpful discussions and advice, Silvia N. Moreno, L. David Sibley, Antonio Barragan, Jean-Francois Dubremetz, Maryse Lebrun, Dominique Soldati-Favre, Gary Ward, Con Beckers, Keith Joiner, Ke Hu, Manami Nishi, and David Roos for providing

antibodies, plasmids, or parasite strains. We also gratefully acknowledge Dhaval Gosalia for his contributions to preliminary experiments, Sharon Reed and Ken Hirata for kindly for providing rTgCPB, Sharada Yadav for making the TgRab7-HA construct, Gary Ward for his patience and support, and the many members of the *Toxoplasma* research community for their input in choosing the name VAC. We thank Claudia Bordon and Tracey Schultz for providing expert technical support and Gary Ward, Anahi Fernandez Cuppari, Björn Kafsack, Silvia N. Moreno and Lois Weisman for critically reading the manuscript, and Marc Pypaert in the Yale Center for Cell and Molecular Imaging for excellent assistance and scientific comments for electron microscopy. This work was supported by grants R01AI060767 (I.C.), R01HL56621 (S.L.D.), and R01AI063263 (V.B.C) from the National Institutes of Health (USA) and grant 04R-796 (V.B.C) from the Stanley Medical Research Institute (USA).

References

Barrett AJ. Cathepsin G. Methods Enzymol. 1981; 80(Pt C):561–565. [PubMed: 7341917]

Binder EM, Lagal V, Kim K. The prodomain of *Toxoplasma gondii* GPI-anchored subtilase TgSUB1 mediates its targeting to micronemes. Traffic. 2008; 9:1485–1496. [PubMed: 18532988]

Botero-Kleiven S, V F. Lindh J, Richter-Dahlfors A, von Euler A, Wahlgren M. Receptor-mediated endocytosis in an apicomplexan parasite (*Toxoplasma gondii*). Exp Parasitol. 2001; 98:134–44. [PubMed: 11527436]

Bradley PJ, Boothroyd JC. The pro region of *Toxoplasma* ROP1 is a rhoptry-targeting signal. Int J Parasitol. 2001; 31:1177–1186. [PubMed: 11513886]

Breinich MS, Ferguson DJ, Foth BJ, van Dooren GG, Lebrun M, Quon DV, et al. A dynamin is required for the biogenesis of secretory organelles in *Toxoplasma gondii*. Curr Biol. 2009; 19:277–286. [PubMed: 19217293]

Brydges SD, Harper JM, Parussini F, Coppens I, Carruthers VB. A transient forward-targeting element for microneme-regulated secretion in *Toxoplasma gondii*. Biol Cell. 2008; 100:253–264. [PubMed: 17995454]

Brydges SD, Sherman GD, Nockemann S, Loyens A, Daubener W, Dubremetz JF, Carruthers VB. Molecular characterization of TgMIC5, a proteolytically processed antigen secreted from the micronemes of *Toxoplasma gondii*. Mol Biochem Parasitol. 2000; 111:51–66. [PubMed: 11087916]

Carey KL, Jongco AM, Kim K, Ward GE. The *Toxoplasma gondii* rhoptry protein ROP4 is secreted into the parasitophorous vacuole and becomes phosphorylated in infected cells. Eukaryot Cell. 2004; 3:1320–30. [PubMed: 15470260]

Carruthers V, Boothroyd JC. Pulling together: An integrated model of Toxoplasma cell invasion. Curr Opin Microbiol. 2007; 10:83–89. [PubMed: 16837236]

Cerede O, Dubremetz JF, Bout D, Lebrun M. The *Toxoplasma gondii* protein MIC3 requires pro-peptide cleavage and dimerization to function as adhesin. EMBO J. 2002; 21:2526–36. [PubMed: 12032066]

Cerede O, Dubremetz JF, Soete M, Deslee D, Vial H, Bout D, Lebrun M. Synergistic role of micronemal proteins in *Toxoplasma gondii* virulence. J Exp Med. 2005; 201:453–463. [PubMed: 15684324]

Desclozeaux M, Venturato J, Wylie FG, Kay JG, Joseph SR, Le HT, Stow JL. Active Rab11 and functional recycling endosome are required for E-cadherin trafficking and lumen formation during epithelial morphogenesis. Am J Physiol Cell Physiol. 2008; 295:C545–56. [PubMed: 18579802]

El Hajj H, Papoin J, Cerede O, Garcia-Reguet N, Soete M, Dubremetz JF, Lebrun M. Molecular signals in the trafficking of *Toxoplasma gondii* protein MIC3 to the micronemes. Eukaryot Cell. 2008; 7:1019–1028. [PubMed: 18390648]

Garcia-Réguet N, Lebrun M, Fourmaux M, Mercereau-Puijalon O, Mann T, Beckers CJM, et al. The microneme protein MIC3 of *Toxoplasma gondii* is a secretory adhesin that binds to both the surface of the host cells and the surface of the parasite. Cell Microbiol. 2000; 2:353–364. [PubMed: 11207591]

Gosalia DN, Salisbury CM, Ellman JA, Diamond SL. High throughput substrate specificity profiling of serine and cysteine proteases using solution-phase fluorogenic peptide microarrays. Mol Cell Proteomics. 2005; 4:626–636. [PubMed: 15705970]

Gu F, Crump CM, Thomas G. Trans-Golgi network sorting. Cell Mol Life Sci. 2001; 58:1067–1084. [PubMed: 11529500]

Harper JM, Zhou XW, V P. Kafsack BF, V C. The novel coccidian micronemal protein MIC11 undergoes proteolytic maturation by sequential cleavage to remove an internal propeptide. Int J Parasitol. 2004; 34:1047–58. [PubMed: 15313131]

Harper JM, Huynh MH, Coppens I, Parussini F, Moreno S, Carruthers VB. A cleavable propeptide influences Toxoplasma infection by facilitating the trafficking and secretion of the TgMIC2-M2AP invasion complex. Mol Biol Cell. 2006; 17:4551–4563. [PubMed: 16914527]

Hoppe HC, Joiner KA. Cytoplasmic tail motifs mediate endoplasmic reticulum localization and export of transmembrane reporters in the protozoan parasite *Toxoplasma gondii*. Cell Microbiol. 2000a; 2:569–578. [PubMed: 11207609]

Hoppe HC, Ngo HM, Yang M, Joiner KA. Targeting to rhoptry organelles of *Toxoplasma gondii* involves evolutionarily conserved mechanisms. Nat Cell Biol. 2000b; 2:449–456. [PubMed: 10878811]

Howell SA, Hackett F, Jongco AM, Withers-Martinez C, Kim K, Carruthers VB, Blackman MJ. Distinct mechanisms govern proteolytic shedding of a key invasion protein in apicomplexan pathogens. Mol Microbiol. 2005; 57:1342–1356. [PubMed: 16102004]

Hu K, Johnson J, Florens L, Fraunholz M, Suravajjala S, DiLullo C, et al. Cytoskeletal components of an invasion machine--the apical complex of *Toxoplasma gondii*. PLoS Pathog. 2006; 2:e13. [PubMed: 16518471]

Huang R, Que X, Hirata K, Brinen LS, Lee JH, Hansell E, et al. The cathepsin L of *Toxoplasma gondii* (TgCPL) and its endogenous macromolecular inhibitor, toxostatin. Mol Biochem Parasitol. 2009; 164:86–94. [PubMed: 19111576]

Huynh MH, Rabenau KE, Harper JM, Beatty WL, Sibley LD, V C. Rapid invasion of host cells by Toxoplasma requires secretion of the MIC2-M2AP adhesive protein complex. EMBO J. 2003; 22:2082–2090. [PubMed: 12727875]

Kawase O, Nishikawa Y, Bannai H, Zhang H, Zhang G, Jin S, et al. Proteomic analysis of calcium-dependent secretion in *Toxoplasma gondii*. Proteomics. 2007; 7:3718–3725. [PubMed: 17880006]

Larson ET, Parussini F, Huynh MH, Giebel JD, Kelley AM, Zhang L, et al. *Toxoplasma gondii* cathepsin l is the primary target of the invasion inhibitory compound LHVS. J Biol Chem . 2009

Manderson AP, Kay JG, Hammond LA, Brown DL, Stow JL. Subcompartments of the macrophage recycling endosome direct the differential secretion of IL-6 and TNFalpha. J Cell Biol. 2007; 178:57–69. [PubMed: 17606866]

Mann T, Beckers C. Characterization of the subpellicular network, a filamentous membrane skeletal component in the parasite *Toxoplasma gondii*. Mol Biochem Parasitol. 2001; 115:257–268. [PubMed: 11420112]

Matrajt M, Donald RG, Singh U, Roos DS. Identification and characterization of differentiation mutants in the protozoan parasite *Toxoplasma gondii*. Mol Microbiol. 2002; 44:735–47. [PubMed: 11994154]

Mitsuda N, Enami K, Nakata M, Takeyasu K, Sato MH. Novel type *Arabidopsis thaliana* H(+)-PPase is localized to the Golgi apparatus. FEBS Lett. 2001; 488:29–33. [PubMed: 11163790]

Molinete M, Irminger JC, Tooze SA, Halban PA. Trafficking/sorting and granule biogenesis in the beta-cell. Semin Cell Dev Biol. 2000; 11:243–251. [PubMed: 10966858]

Montalvetti A, Rohloff P, Docampo R. A functional aquaporin co-localizes with the vacuolar proton pyrophosphatase to acidocalcisomes and the contractile vacuole complex of *Trypanosoma cruzi*. J Biol Chem. 2004; 279:38673–38682. [PubMed: 15252016]

Mullock BM, Bright NA, Fearon CW, Gray SR, Luzio JP. Fusion of lysosomes with late endosomes produces a hybrid organelle of intermediate density and is NSF dependent. J Cell Biol. 1998; 140:591–601. [PubMed: 9456319]

Ngo HM, Yang M, Paprotka K, Pypaert M, Hoppe H, Joiner KA. AP-1 in *Toxoplasma gondii* mediates biogenesis of the rhoptry secretory organelle from a post-golgi compartment. J Biol Chem. 2003; 278:5343–52. [PubMed: 12446678]

Nichols BA, Chiappino ML, Pavesio CE. Endocytosis at the micropore of *Toxoplasma gondii*. Parasitol Res. 1994; 80:91–98. [PubMed: 8202461]

Norrby R, Lindholm L, Lycke E. Lysosomes of *Toxoplasma gondii* and their possible relation to the host-cell penetration of Toxoplasma parasites. J Bacteriol. 1968; 96:916–9. [PubMed: 4176646]

Opitz C, Di Cristina M, Reiss M, Ruppert T, Crisanti A, Soldati D. Intramembrane cleavage of microneme proteins at the surface of the apicomplexan parasite *Toxoplasma gondii*. EMBO J. 2002; 21:1577–85. [PubMed: 11927542]

Pelletier L, Stern CA, Pypaert M, Sheff D, Ngo HM, Roper N, et al. Golgi biogenesis in *Toxoplasma gondii*. Nature. 2002; 418:548–52. [PubMed: 12152082]

Pfeffer SR. Rab GTPases: Specifying and deciphering organelle identity and function. Trends Cell Biol. 2001; 11:487–491. [PubMed: 11719054]

Que X, Ngo H, Lawton J, Gray M, Liu Q, Engel J, et al. The cathepsin B of *Toxoplasma gondii*, toxopain-1, is critical for parasite invasion and rhoptry protein processing. J Biol Chem. 2002; 277:25791–7. [PubMed: 12000756]

Rabenau KE, Sohrabi A, Tripathy A, Reitter C, Ajioka JW, Tomley FM, V C. TgM2AP participates in *Toxoplasma gondii* invasion of host cells and is tightly associated with the adhesive protein TgMIC2. Mol Microbiol. 2001; 41:537–47. [PubMed: 11532123]

Robibaro B, Stedman TT, Coppens I, Ngo HM, Pypaert M, Bivona T, et al. *Toxoplasma gondii* Rab5 enhances cholesterol acquisition from host cells. Cell Microbiol. 2002; 4:139–152. [PubMed: 11906451]

Rodriguez-Boulan E, Musch A. Protein sorting in the Golgi complex: Shifting paradigms. Biochim Biophys Acta. 2005; 1744:455–464. [PubMed: 15927284]

Salisbury CM, Maly DJ, Ellman JA. Peptide microarrays for the determination of protease substrate specificity. J Am Chem Soc. 2002; 124:14868–14870. [PubMed: 12475327]

Schrader M. Membrane targeting in secretion. Subcell Biochem. 2004; 37:391–421. [PubMed: 15376628]

Shaw MK, Roos DS, Tilney LG. Acidic compartments and rhoptry formation in *Toxoplasma gondii*. Parasitology. 1998; 117:435–443. [PubMed: 9836308]

Sinai AP. Biogenesis of and activities at the *Toxoplasma gondii* parasitophorous vacuole membrane. Subcell Biochem. 2008; 47:155–164. [PubMed: 18512349]

Sobo K, Chevallier J, Parton RG, Gruenberg J, van der Goot FG. Diversity of raft-like domains in late endosomes. PLoS One. 2007; 2:e391. [PubMed: 17460758]

Stow JL, Ching Low P, Offenhauser C, Sangermani D. Cytokine secretion in macrophages and other cells: Pathways and mediators. Immunobiology . 2009

Turk B, V T. Turk D. Structural and functional aspects of papain-like cysteine proteinases and their protein inhibitors. Biol Chem. 1997; 378:141–50. [PubMed: 9165064]

Weisman LS. Organelles on the move: Insights from yeast vacuole inheritance. Nat Rev Mol Cell Biol. 2006; 7:243–252. [PubMed: 16607287]

Wilkin MB, Carbery AM, Fostier M, Aslam H, Mazaleyrat SL, Higgs J, et al. Regulation of notch endosomal sorting and signaling by drosophila Nedd4 family proteins. Curr Biol. 2004; 14:2237–2244. [PubMed: 15620650]

Woodman PG, Futter CE. Multivesicular bodies: Co-ordinated progression to maturity. Curr Opin Cell Biol. 2008; 20:408–414. [PubMed: 18502633]

Yang M, Coppens I, Wormsley S, Baevova P, Hoppe HC, Joiner KA. The *Plasmodium falciparum* Vps4 homolog mediates multivesicular body formation. J Cell Sci. 2004; 117:3831–3838. [PubMed: 15252121]

Zhen RG, Kim EJ, Rea PA. Localization of cytosolically oriented maleimide-reactive domain of vacuolar H(+)-pyrophosphatase. J Biol Chem. 1994; 269:23342–23350. [PubMed: 8083239]

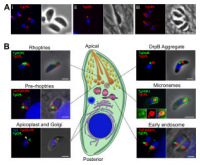

Fig. 1. TgCPL occupies a novel apical organelle

A. TgCPL localization in formaldehyde fixed RH parasites by immunofluorescence using MαTgCPL showing that TgCPL occupies a single apical localization in extracellular (i) and newly invaded parasites (ii). In contrast, TgCPL showed a punctate distribution in tachyzoites undergoing intracellular replication (iii).

B. Dual staining of TgCPL with previously defined exocytic and endocytic markers. Parasites were stained with antibodies to TgROP2 (rhoptries), proTgROP4 (prerhoptry), TgGRASP-mRFP (Golgi cisternae), TgDrpB (cytoplasmic aggregate), TgAMA1 (micronemes), or TgRab51HA (EE). For the parasite illustration, the cytoplasm and pellicular membranes (plasma membrane and inner membrane complex) are shown in shades of green, DNA containing structures (nucleus and apicoplast) are blue, the early exocytic pathway (ER and Golgi) is shown in shades of purple, the endocytic system (EE, LE, and VAC) in shades of pink, and the late exocytic system in shades of orange-yellow. Scale bar, 2μm.

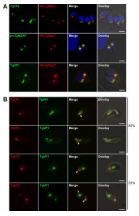

Fig. 2. The VAC is juxtaposed to the LE, which contain proTgM2AP and TgVP1

A. RH parasites were transiently transfected with a plasmid expressing the LE marker TgRab7HA and intracellular parasites were fixed and processed for IFA 24 h post-transfection.

B. Dual staining of TgCPL and TgVP1 in extracellular tachyzoites. TgCPL is concentrated in the VAC along with some TgVP1 (arrowhead) in most parasites. TgVP1 additionally occupies sites that are often adjacent to the VAC and in some cases also contain a minority population of TgCPL (arrow). Scale bar, 2 mm.

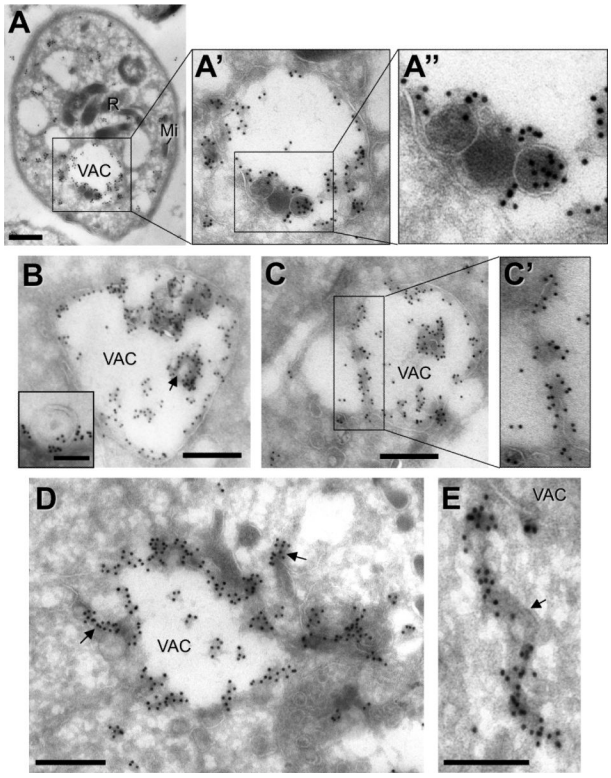

Fig. 3. Ultrastructure of the VAC

Extracellular tachyzoites were immunolabeled with MαTgCPL antibodies before incubation with 10 nm protein A-gold particles.

A. A globoid VAC surrounded by a single membrane containing TgCPL is observed in the apical area enriched in micronemes (Mi) and rhoptries (R). Magnifications (**A', A''**) reveal the presence of intraluminal vesicles with dense core material.

B and **inset.** Internal vesicles delineated by a double membrane (arrow) are visible that may be the result of engulfment of an incoming vesicle by the VAC.

C and **C'.** Deep invaginations of the VAC limiting membrane.

D. Outward deformation of the multivesicular endosomal membrane.

E. Tubulovesicular structures decorated by TgCPL may either result from the budding of the limiting membrane of the VAC or correspond to endosomal tubules fusing with the VAC.

Scale bars are 200 nm, except 100 nm in inset in **C**.

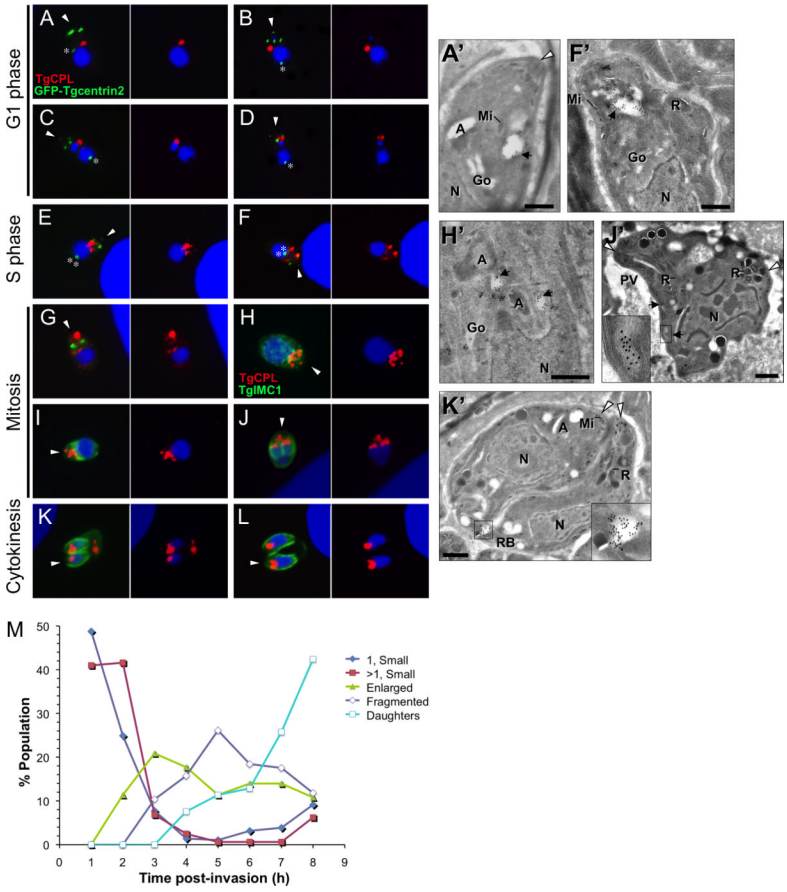

Fig. 4. Dynamic fragmentation of the VAC during intracellular replication

TgCPL distribution during intracellular replication was studied by staining EGFP-Centrin2 expressing parasites with RαTgCPL and MαGFP (to enhance the signal) (**A-G**) or RH parasites with MαTgCPL and RαTgIMC1 (**H-L**). Infected host cells were fixed at 1 h intervals 1-8 h post-invasion. The apical end of the parasite is indicated with an arrowhead and the centrosome is marked with an asterisk.

A', **F**', **H**', **J'** and **K**'. Cryoimmunoelectron micrographs of MαTgCPL immunogold (10 nm) staining of intracellular tachyzoites in different stages of endodyogeny. Apicoplast, A; Golgi, Go; Rhoptry, R; Microneme, Mi; Nucleus, N, Parasitophorous Vacuole, PV; Residual Body, RB; VAC, black arrowhead; Apical tip of the parasites, white arrowhead. See text for descriptions. Scale bars, 200 nm.

M. Quantification of TgCPL staining patterns during parasite replication. Data shown are the combined results of three independent experiments.

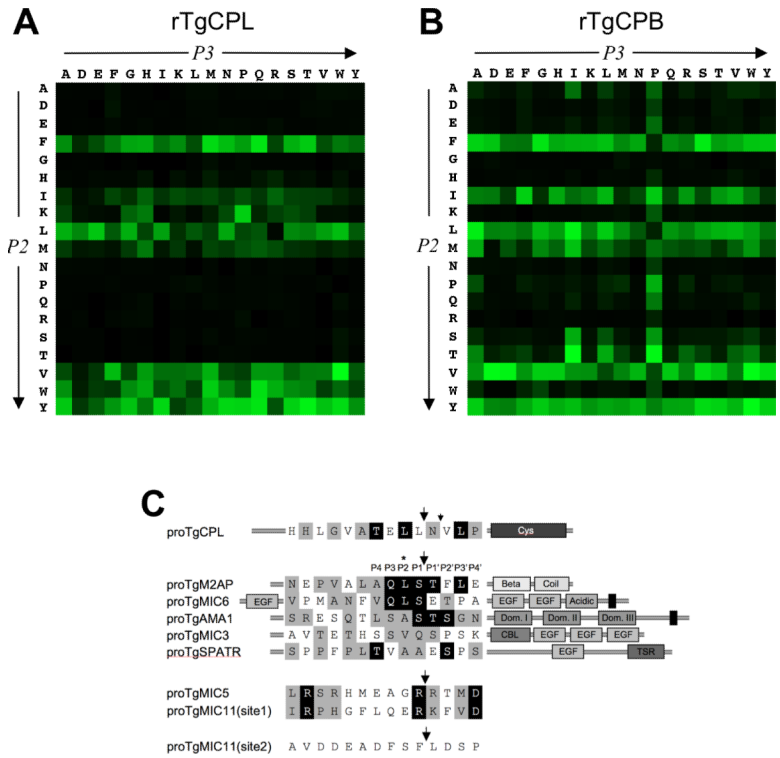

Fig. 5. rTgCPL cleavage specificity is consistent with the propeptide cleavage site of several proMICs

A-B. Mapping P2 and P3 cleavage specificities of TgCPL and TgCPB. rTgCPL and rTgCPB (10 nM each) were screened against a Ala-P3-P2-Arg-ACC peptide substrate library (10μM) with all possible combinations of natural amino acids (except Cys) at the P2 and P3 positions (Salisbury *et al.*, 2002; Gosalia *et al.*, 2005). Initial rate velocities were measured by fluorescence in 384-well plates and are displayed as a heat map with color intensity indicating the rate of cleavage. Note that the strong preference of rTgCPB for P3 Pro might not be accurately indicated for peptides also having a highly preferred P2 residue (Phe, Leu, Val) because these reactions may have proceeded so quickly that they reached plateau phase before values could be measured. The experiment was performed three times with consistent results.

C. Alignment of the r100proTgCPL autocleavage site with the propeptide cleavage sites of proMICs. Sequences were manually aligned (without gaps) with respect to the principal propeptide cleavage site (large arrow). A minor cleavage site of r100proTgCPL is also shown (small arrow). Identical residues within each group are shown in black boxes and similar residues are shown in grey boxes. Similar amino acids were classified as: non-polar (G, A, V, L, M, I); aromatic (F, Y, W); polar, uncharged (S, T, C, P, N, Q); polar, positively charged (K, R, H); or polar, negatively charged (D, E). TgMIC11 has an internal propeptide that is excised by two cleavage events at site 1 and site 2 (Harper *et al.*, 2004). Protein domains are as follows: EGF, epidermal growth factor; Dom. I, domain I; Dom. II, domain II, Dom. III, domain III; CBL, chitin binding-like; TSR, thrombospondin repeat; Cys, cysteine protease. Transmembrane anchors are illustrated as black rectangles. Domain structures of TgMIC5 and TgMIC11 are unknown since they lack homology to other proteins. The P2 position of the proMIC propeptide cleavage sites is marked with an asterisk to indicate the highest level of conservation. Cleavage sites were defined in the following studies: TgM2AP (Rabenau *et al.*, 2001), TgMIC6 (Opitz *et al.*, 2002), TgAMA1 (Howell *et al.*, 2005), TgMIC3 (Garcia-Réguet *et al.*, 2000), TgSPATR (Kawase *et al.*, 2007),

r100proTgCPL (present study), TgMIC5 (Brydges *et al.*, 2000), TgMIC11 (Harper *et al.*, 2004).

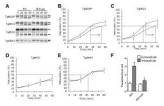

Fig. 6. TgCPL-deficient parasites show impaired maturation of proTgM2AP and proTgMIC3, and are defective in cell invasion

A. Pulse metabolically labeled RH or RHΔ*cpl* parasites were either kept on ice (0 min) or chased with medium containing unlabelled Met/Cys for the indicated times. MIC proteins were immunoprecipitated and analyzed by SDS-PAGE and autoradiography. Arrows indicate positions of the immature (upper) and mature (lower) forms of each MIC protein.

B-**E**. Quantification of MIC maturation in RH (squares) and RHΔ*cpl* (circles) parasites is shown. Values are mean±s.d. of three (TgMIC6, TgAMA1), five, (TgMIC3), or six (TgM2AP) experiments and were calculated as described in figure legend 4.

F. RHΔ*cpl* parasites are less invasive than RH parasites. Parasites were allowed to invade HFF cells for 30 min prior to fixation. Extracellular parasites were stained with RαTgSAG1 before permeabilization and staining of intracellular parasites with a monoclonal antibody to TgSAG1.

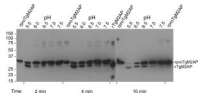

Fig. 7. rTgCPL correctly processes rproTgM2AP in a low pH dependent manner

A. Immunoblot probed with rabbit α-His tag showing a pH dependent TgM2AP propeptide cleavage mediated by rTgCPL. Affinity purified rproTgM2AP (400 ng) was incubated with rTgCPL (40 ng) at each pH value for the indicated times at 37°C. Note the low pH and time dependent production of a band that comigrates with rTgM2AP.

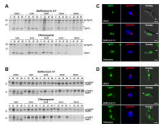

Fig. 8. *In vivo* maturation of proTgCPL and proTgM2AP are differentially sensitive to pH antagonists

A. Representative autoradiographs showing inhibition of processing in parasite treated with pH-altering substances. RH parasites were pretreated for 15 min with the indicated concentrations of bafilomycin A1 or chloroquine before pulse labeling with [^{35}S] Met/Cys for 10 min, chasing for the indicated times, and immunoprecipitation with Rαr100TgCPL. Asterisks indicate intermediate processed forms (48 kDa and 32 kDa) of proTgCPL.

B. Same as **A** except immunoprecipitations were performed with RαrTgM2AP and mAb T4.2F3 against TgMIC3. Molecular weight markers are expressed in kDa.

C. Bafilomycin A1 and chloroquine induced enlargement of the VAC. Representative immunofluorescence images showing TgCPL localization in RH parasites expressing TgGRASP-mRFP after treatment with pH antagonists. Parasites were treated with DMSO (upper panel); 500 nM bafilomycin A1 (middle panel); or 150 μM chloroquine (lower panel) for 15 min at RT, and then incubated for another 1h at 37°C.

D. Bafilomycin A1 and chloroquine induced swelling and disassembling of the LE. Representative immunofluorescence images showing TgVP1 localization in RH parasites expressing TgGRASP-mRFP after treatment with DMSO (upper panel); 500 nM bafilomycin A1 (middle panel); or 150 μM chloroquine (lower panel) as described above. Arrowheads indicate the apical end of the parasite.

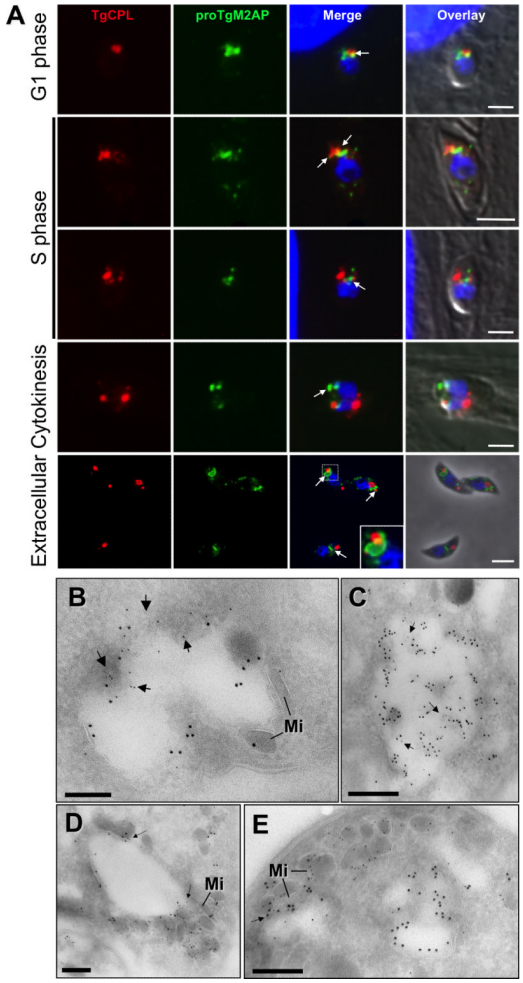

Fig. 9. TgCPL and proTgM2AP encounter each other in microdomains along the endo/exocytic pathway

A. Dual staining of TgCPL and proTgM2AP during daughter cell formation was studied in fixed intracellular (G1, S, M) or extracellular (E) RH parasites by double immunolocalization using MαTgCPL and RαproTgM2APpep. TgCPL and proM2AP are located on adjacent dynamic compartments with small areas or microdomains where the overlap is evident at different stages of daughter cell formation. Arrows indicate the areas where small amounts of TgCPL have access to proTgM2AP. The inset is a higher magnification of the region indicated by dotted frames.

B-E. Double cryoimmunoelectron microscopy of extracellular tachyzoites immunolabeled with anti-TgCPL (revealed with protein A-gold particles of 10 nm), and anti-proTgM2AP (**C**; 5 nm gold) or anti-TgM2AP.

D, E, and **F**. (5 nm gold). Arrows pinpoint the co-distribution of TgCPL and proTgM2AP. Also note the concentration of micronemes (Mi) containing TgCPL and TgM2AP around the VAC (panels **E** and **F**). Scale bars are 100 nm.

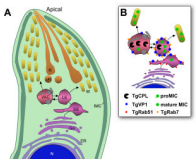

Fig. 10. Hypothetical model of trafficking and maturation in the endo/exocytic pathway

A. The model indicates that MIC protein complexes are synthesized in the ER before transiting through the Golgi apparatus and a series of post-Golgi endosomal compartments including the EE, the LE, and possibly the VAC. Rather than the TGN being the sorting station from where the budding of immature secretory granules primarily occurs as in higher eukaryotes, our model proposes that micronemes are formed by budding from an endocytic compartment, either the LE or the VAC. Dashed lines indicate possible alternative routing of proTgCPL from the ER or Golgi to the VAC.

B. The model further proposes that proteolytic maturation of proMICs mediated by TgCPL and other proteases occurs within these compartments and possibly also in nascent micronemes. Acidification of the intralumenal environment of both compartments could be an important endogenous factor modulating the autoactivation of proTgCPL and limited proteolysis by TgCPL or alternative maturases.

Table 1

Half times of microneme protein maturation in RH and RHΔ*cpl* strains

MIC	Strain	$T_{1/2}$ (min)						Ave±s.d.	t-test
		1[a]	2	3	4	5	6		
TgM2AP	RH	37.7	38.9	34.9	42.0	40.3	39.8	38.9±2.4	
	RHΔ*cpl*	51.5	58.1	48.8	60.0	59.5	57.8	56.0±4.6	p=0.000014*
TgMIC3	RH	37.2	38.3	ND[b]	34.7	34.0	34.3	35.7±1.9	
	RHΔ*cpl*	56.6	56.0	ND	41.5	44.5	40.0	47.7±8.0	p=0.013*
TgAMA1	RH	32.0	33.4	30.8	ND	ND	ND	32.1±1.3	
	RHΔ*cpl*	37.2	24.6	31.8	ND	ND	ND	31.2±6.3	p=0.854
TgMIC6	RH	>60[c]	>60	>60	ND	ND	ND	>60	
	RHΔ*cpl*	>60	>60	>60	ND	ND	ND	>60	NA[d]
TgMIC5	RH	11.2	13.3	9.9	ND	ND	ND	11.5±1.7	
	RHΔ*cpl*	12.9	13.8	11.9	ND	ND	ND	12.9±1.0	p=0.093

[a] Experiment number

[b] ND, not determined

[c] Processing did not reach 50% within the 60 min time period of the experiment

[d] NA, not applicable

* $p < 0.05$

Mol Microbiol. Author manuscript; available in PMC 2011 June 1.